invitrogen

Two data sets. One step. Zero doubt.

Confidently confirm your cell profiles with a new flow cytometer that delivers flow cytometry and imaging data simultaneously. Now, you can acquire dual data quickly and easily. The new Invitrogen™ Attune™ CytPix™ Flow Cytometer delivers both brightfield images and flow cytometry data sets simultaneously, so you can confirm cellular characteristics and sample quality confidently, without changing your protocols.

Enhance analysis and confidence at **thermofisher.com/cytpix**

ThermoFisher SCIENTIFIC

DOI: 10.1002/JLB.1HI0621-313R

JLB JOURNAL OF LEUKOCYTE BIOLOGY

HIGHLIGHTED ARTICLE

Kindlin-3 maintains marginal zone B cells but confines follicular B cell activation and differentiation

Andrea Härzschel[1,2] | Lixia Li[1] | Peter W. Krenn[3,4] | Eva Szenes-Nagy[2] | Geoffroy Andrieux[5,6] | Elisabeth Bayer[2] | Dietmar Pfeifer[1] | Laura Polcik[1] | Ursula Denk[2] | Jan P. Höpner[2] | Elif Karabatak[1] | Danielle-Justine Danner[1] | Simone Tangermann[7] | Lukas Kenner[7,8,9,10] | Hassan Jumaa[11] | Richard Greil[2] | Melanie Börries[5,6] | Raphael Ruppert[3] | Palash C. Maity[11] | Tanja Nicole Hartmann[1]

[1] Department of Internal Medicine I, Faculty of Medicine and Medical Center, University of Freiburg, Freiburg, Germany

[2] Department of Internal Medicine III with Hematology, Medical Oncology, Hemostaseology, Infectiology and Rheumatology, Oncologic Center, Salzburg Cancer Research Institute - Laboratory for Immunological and Molecular Cancer Research (SCRI-LIMCR), Paracelsus Medical University, Cancer Cluster Salzburg, Salzburg, Austria

[3] Max Planck Institute of Biochemistry, Martinsried, Germany

[4] Department of Biosciences, Cancer Cluster Salzburg, Paris-Lodron University of Salzburg, Salzburg, Austria

[5] Institute of Medical Bioinformatics and Systems Medicine, Medical Center-University of Freiburg, Faculty of Medicine, University of Freiburg, Freiburg, Germany

[6] German Cancer Consortium (DKTK) and German Cancer Research Center (DKFZ), Heidelberg, Germany

[7] Unit of Laboratory Animal Pathology, University of Veterinary Medicine, Vienna, Austria

[8] Department of Clinical Pathology, Medical University Vienna, Vienna, Austria

[9] Department of Experimental Pathology and Laboratory Animal Science, Medical University of Vienna, Vienna, Austria

[10] Ludwig Boltzmann Institute for Cancer Research, Vienna, Austria

[11] Institute of Immunology, Ulm University, Ulm, Germany

Correspondence
Tanja Nicole Hartmann, Department of Internal Medicine I, Faculty of Medicine and Medical Center, University of Freiburg, Freiburg, Germany.
Email: tanja.hartmann@uniklinik-freiburg.de

Abstract

Integrin-mediated interactions between hematopoietic cells and their microenvironment are important for the development and function of immune cells. Here, the role of the integrin adaptor Kindlin-3 in B cell homeostasis is studied. Comparing the individual steps of B cell development in B cell-specific Kindlin-3 or alpha4 integrin knockout mice, we found in both conditions a phenotype of reduced late immature, mature, and recirculating B cells in the bone marrow. In the spleen, constitutive B cell-specific Kindlin-3 knockout caused a loss of marginal zone B cells and an unexpected expansion of follicular B cells. Alpha4 integrin deficiency did not induce this phenotype. In Kindlin-3 knockout B cells VLA-4 as well as LFA-1-mediated adhesion was abrogated, and short-term homing of these cells in vivo was redirected to the spleen. Upon inducible Kindlin-3 knockout, marginal zone B cells were lost due to defective retention within 2 weeks, while follicular B cell numbers were unaltered. Kindlin-3 deficient follicular B cells displayed higher IgD, CD40, CD44, CXCR5, and EBI2 levels, and elevated PI3K

Abbreviations: BCR, B cell receptor; BM, bone marrow; FO, follicular; GC, germinal center; GEO, gene expression omnibus; GSEA, geneset enrichment analysis; Iv, intravenous; K3, kindlin-3; LFA-1, lymphocyte function-associated antigen-1; MFI, mean fluorescence intensity; MZ, marginal zone; PB, peripheral blood; TFH, follicular helper T cells; VLA-4, very late antigen-4; wt, wildtype

signaling upon CXCR5 stimulation. They also showed transcriptional signatures of spontaneous follicular B cell activation. This activation manifested in scattered germinal centers in situ, early plasmablasts differentiation, and signs of IgG class switch.

KEYWORDS
B cell activation, CXCR5, follicular B cells, Integrin adhesion, marginal zone B cells

1 | INTRODUCTION

The correct differentiation of B cells requires their appropriate localization to distinct organs, zones, and signals in a sequential process. Integrins support leukocyte development and differentiation by orchestrating cell extravasation from the blood circulation and retention within the hematopoietic organs. The two major integrins expressed on B cells are the heterodimers alpha4beta1 ($\alpha4\beta1$, a.k.a. very late Ag-4 (VLA-4), CD49d/CD29) and $\alpha L\beta2$ (lymphocyte function-associated antigen-1 (LFA-1), CD11a/CD18).[1] VLA-4 is thought to be essential for the interaction of early B cell progenitors with the bone marrow (BM) niche, mediating their adhesion to stromal elements expressing the VLA-4 ligand VCAM-1,[2,3,4] whereas LFA-1 is considered to predominantly orchestrate the interactions of differentiated B cells within lymph nodes. Both LFA-1 and VLA-4 might contribute to efficient Ag acquisition of B cells and their subsequent activation.[5,6]

The ligand-binding function of integrins requires their transition from a low into a high-affinity conformation. This transition, triggered by the so-called inside-out integrin activation cascade, allows rapid and dynamic changes in integrin-mediated cell adhesion. The process is initiated by cell surface receptors such as chemokine receptors, the B cell receptor (BCR), or CD44 that bind chemokines, Ags, or hyaluronic acid, respectively,[7–9] and subsequently involves several kinases to activate the integrin. The high-affinity conformation of the integrin is stabilized by at least two types of intracellular integrin adaptors, talins and kindlins, which bind independently to different motifs in the cytoplasmic tail of β integrin subunits.[10,11]

The kindlin family comprises three members, namely Kindlin-1, Kindlin-2, and Kindlin-3 (K3), with K3 being exclusively expressed in the hematopoietic system.[12] Hematopoietic stem- and progenitor cells, T-cells, neutrophils and platelets require K3-mediated integrin activation for their correct positioning and function.[13–16] It has not yet been studied, whether K3 plays a role in the differentiation of normal B cells or their malignant counterparts, which are highly dependent on VLA-4 activation,[9,17] and elucidation of the function of K3 in B cells might bring new insights into mechanisms not only of lymphomagenesis but also of autoimmunity.

Here, we used the mb1 Cre transgene to create mouse strains harboring a K3 or CD49d/VLA-4 deletion in pre-pro B cells and all later stages.[18] We identified the requirement of K3 for both, VLA-4 and LFA-1 activation and found distinct K3 and VLA-4 roles in controlling immature B cells and maintaining marginal zone B cells. K3 loss induced follicular (FO) B cell activation and increased CXCR5 responsiveness resulting in proliferation and de novo scattered germinal centers and plasmablast differentiation.

2 | METHODS

2.1 | Study approvals and mice

All mouse experiments were approved by the animal ethics committees. Fermt3 (K3) floxed (fl/fl) (Fermt3tm2.1Ref) mice[19] were obtained from Reinhard Fässler, Martinsried, Germany, ITGA4 (CD49d) floxed (Itga4tm1Tpa) mice[20] from Thalia Papayannopoulou, Washington, USA, and mb1 Cre (Cd79atm1(cre)Reth) mice[18] from Michael Reth, Freiburg, Germany. Tamoxifen–inducible Cre mice (B6.129-Gt(ROSA)26Sortm1(cre/ERT2)Tyj/J) and Cre reporter mice (Gt(ROSA)26Sortm4(ACTB-tdTomato,-EGFP)Luo/J) were purchased from Jackson Laboratories. All strains were backcrossed to C57BL/6J. Mice were sacrificed for analysis at the age of 8–12 weeks. For negative selection of B cells, Pan B cell isolation kit II (Miltenyi) or EasySep mouse pan B cell isolation kit (Stem cell Technologies) was used. Purity was confirmed to be >90% by flow cytometry. For all experiments, fl/fl littermates expressing no Cre were used as wildtype (wt) controls.

2.2 | Flow cytometry

For B cell subset determination, single-cell suspensions were prepared from freshly isolated organs. Integrins and chemokine receptors were labeled at 4°C and B cell subset markers at room temperature prior to detection by flow cytometry (Gallios, Beckman Coulter, and Fortessa, BD). Absolute cell numbers were determined by flow cytometry using Flow-Count-Fluorospheres (Beckman Coulter) or the EVE automatic cell counter (NanoEnTek). Analysis was performed using Kaluza (Beckman Coulter) or FlowJo (BD Bioscience).

2.3 | Immunofluorescence

Spleens were frozen in TissueTek (Miles Laboratories) and stored at −80°C before cutting them to 10-μm cryostat sections. Sections were fixed in methanol, blocked using 1% BSA, and incubated with primary Abs at 4°C, followed by respective secondary Abs. Primary Abs

were directed against laminin (Novus), B220 (BD), Ki67 (R&D systems), Moma1 (Abcam), IgM (Southern Biotech), GL7 (Biolegend), and IgG (AbD Serotec, house biotinylated). Corresponding secondary Abs were donkey anti-rabbit Alexa 647-conjugated IgG (Dianova), donkey anti-rat Alexa565-conjugated IgG (Abcam), donkey anti-sheep Alexa 488-conjugated IgG (Dianova), and Streptavidin-Dylight 594 (Vector Lab). Sections were mounted using antifade mounting medium containing DAPI (Biozol) and were examined using a 20× PL ApoChromat objective (numerical aperture 0.8) and an Axioimager microscope (Zeiss) with an Axiocam 506 mono-color camera, or a confocal laser scanning microscope LSM 710 with motorized stage (Zeiss). Images were acquired by Zen software (Zeiss) and analyzed using Image J (NIH).

2.4 | Adoptive transfer

Up to 15 × 10^6 splenocytes from K3 fl/fl Cre reporter mice with or without mb1 Cre expressing GFP/dTomato (K3 deficient- and control cells, respectively) were injected intravenously (i.v.) into C57BL/6J wt mice (Janvier Laboratories). The absolute injected cell number was determined by flow cytometry using FlowCount Fluorospheres (Beckman Coulter). After 3 h, mice were sacrificed, single-cell suspensions of the organs were prepared and the number of recovered donor cells was determined by flow cytometry. The normalized cell recovery rate was calculated as GFP/dTomato positive cells/10^6 of murine host cells/10^6 cells injected as described before.[21,22]

2.5 | Real-time analysis of VLA-4 affinity

Real-time flow cytometry of VLA-4 affinity was performed as described.[23] The autofluorescence baseline of purified splenic B cells was determined using an Accuri flow cytometer (BD Biosciences). After 1 min measurement, the small molecule VLA-4 ligand LDV-FITC was added to the sample and the fluorescence intensity was recorded for an additional 2 min. Then, CXCL12 (100 ng/ml), CXCL13 (500 ng/ml) or anti-IgM $F(ab)_2$ (10 μg/ml) was added. After another 2 min, unlabeled LDV was added in excess. Measurement continued for further 3 minutes. The dissociation rate constant (K_{off}), was obtained by fitting the data to a one-phase exponential decay equation. The ligand residence time was calculated as $1/K_{off}$ as described.[24]

2.6 | In vitro shear flow assay

Shear flow assays were performed as previously described.[17,22] Plates were coated with protein A followed by immobilization of VCAM-1-Fc or ICAM-1-Fc and subsequent overlay with chemokine (CXCL12). Shear stress was generated with an automated syringe pump attached to the outlet side of a parallel laminar flow chamber (6-channel μ-slides, Ibidi). Purified splenic B cells were perfused in the flow chamber, the entire perfusion period was recorded and digitalized. Analysis of the video-recorded segments was performed using a customized software (WIMASIS). Frequencies of adhesive categories were determined as percentages of cells flowing immediately over the substrates.

2.7 | Tamoxifen treatment

Tamoxifen (5 mg; Sigma-Aldrich) per mouse was administered orally to 8-10-week-old Fermt3fl/fl RosaCreERT2 mice on 2 consecutive days. Blood was taken 1 week after tamoxifen administration; mice were sacrificed 2 weeks after administration. Marginal zone and follicular B cells were quantified by flow cytometry.

2.8 | Transcriptome analysis

Clariome D assay (Affymetrix) was performed on RNA of sorted splenic follicular B cells ($CD19^+/B220^+/IgM^+/CD21^{low}$) from 10-week-old K3ΔB mice and control littermates. Normalized RNA intensity was obtained after Robust Multichip Average (RMA) normalization using the oligo R package.[25] Differential expression analysis between K3ΔB and control mice was performed with the linear model-based approach, limma R package.[26] P-value, adjusted with Benjamini Hochberg (BH) method, below 0.05 was set as the significance threshold. Genes were ranked according to the log2 foldchange in K3ΔB versus control and used as input in a gene-set enrichment analysis with the fgsea R package. MSigDB was used as gene-sets.[27,28] BH *P*-value below 0.05 was set as significance threshold. Transcriptome data are available at Gene Expression Omnibus (GEO), accession number: GSE172080 (access token: clsncsmqxpkzhin).

2.9 | Phosphoflow

Viable cells from spleens were identified using fixable viability dye eFluor 780 (Thermo Fisher). Following stimulation at 37°C by CXCL13 (500 ng/ml; R&D) or α-IgD (10 μg/ml) in RPMI containing 0.5% BSA for 5 min, the cells were immediately fixed with pre-warmed Fix solution (BD PhosFlow, Fix buffer 1) at 37°C for 10 min and subsequently permeabilized with 90% methanol for 10 min on ice. Phosphorylation of AKT in follicular B cells was then determined by co-staining the cells using anti-pAKT(S473), CD19, CD24, and CD21 Abs.

2.10 | Chemotaxis assay

Freshly isolated splenocytes were subjected to Boyden chamber transwells (Corning, 5 μm pore size) for 2 h, with the lower well-containing medium alone (control) or medium containing CXCL12 (100 ng/ml) or CXCL13 (500 ng/ml). Chemotaxis was cytometrically quantified using flow counting beads; B cells were identified by CD19 staining.

2.11 | Calcium mobilization assay

Whole splenocytes were labeled with Fluo-3-AM (Thermo Fisher) and subsequently stained on ice with Abs against B220, CD24, and CD21, allowing for the identification of follicular B cells. Prior to measurement, cells were warmed to 37°C. Fluorescence was acquired for 3 min on BD Cytoflex at 37°C. After one minute, the stimuli (anti-IgM (10 μg/ml), anti-kappa (10 μg/ml), anti-IgD (10 μg/ml), CXCL12 (100 ng/ml), or CXCL13 (500 ng/ml) were added. Fluorescence over time was plotted using FlowJo, and the area under the curve was determined graphically using ImageJ.

2.12 | Polarization analysis

B cells from spleens were isolated by negative selection to purity >90% and seeded on chamber slides coated with either Collagen I (Ibidi) alone or co-coated with CXCL12 or CXCL13 and allowed to adhere in HBSS containing 0.5% BSA, 1 mM $CaCl_2$, and $MgCl_2$ for 30 min. The cells were then fixed and stained with Phalloidin-AF488 (Thermo Fisher). Images were taken by an MRm mono-color camera at 20× PL NeoFluar objective (numerical aperture 0.5) of an AxioObserver.Z1 (Zeiss) using Zen software (Zeiss). Cellular polarization was classified according to the pattern of phalloidin staining and analyzed using Image J (NIH).

2.13 | Statistical analysis

Statistical analysis was performed with GraphPad Prism 5. Normal distribution was tested for all datasets. Normally distributed groups were compared using unpaired or paired *t*-test, not-normally distributed data sets using Mann-Whitney or Wilcoxon matched-pairs signed-rank test. Significance threshold was $P < 0.05$, with values at $P < 0.05$ marked as *, $P < 0.01$ as **, and $P < 0.001$ as ***.

3 | RESULTS

3.1 | K3 as well as CD49d expression are required to maintain immature and mature B cells in the bone marrow

We intercrossed mice expressing the Cre-recombinase under the control of the mb1 (CD79a) promoter[18] with Fermt3 (K3) fl/fl mice and ITGA4 (CD49d) fl/fl mice, thereby establishing mice harboring a K3 knockout or a CD49d knockout specifically in all B cells (Supplemental Fig. 1A and B). Then, we compared the distribution of different B cell subsets in the organs of these mice (hereafter called K3ΔB mice and CD49dΔB mice) with their respective wt littermates by flow cytometry (for gating strategies see Figure 1A). An overview of the marker expression during B cell development is shown in Supplemental Fig. 1C. An example for the gating of BCR negative subpopulations is shown in Supplemental Fig. 1D. Despite the efficient mb1 Cre-based knockout from very early B cell stages on,[18] mice from both conditional knockout strains did not differ from littermate controls in their number of early (BCR negative) and IgM low immature B cells (Figure 1B,C_i). However, numbers of immature IgM^{high}/IgD^{neg} were in tendency reduced in K3ΔB mice ($P = 0.05$) and significantly reduced in CD49dΔB mice (Figure 1C_{ii}). In both knockout conditions, IgM^{high}/IgD^{int} B cells were reduced (Figure 1 C_{iii}). The most striking change observed in both K3ΔB and CD49dΔB mice compared to wt littermates was a loss of IgM^{high}/IgD^{high} B cells, which comprise the recirculating, mature B cell subset (Figure 1D). As the CXCL12-CXCR4 axis controls B lineage cell movement within BM,[29] we next analyzed the migratory behavior of the B cell subsets in detail, including BCR negative B cell subpopulations (Pre-Pro-, Pro-, and Pre B cells). We observed that upon K3 loss, chemotaxis towards CXCL12 was decreased in all B cell subsets except the very earliest ones (Pre-Pro-, Pro-, and Pre B cells; Supplemental Fig. 1E), proposing migration defects as a potential mechanism for the loss of the later, IgD positive B cell subsets. Total B cell numbers in BM as well as the percentage of B cells among lymphocytes was unaltered in K3ΔB and CD49dΔB mice compared to wt controls (Supplemental Fig. 1F).

3.2 | Upon Kindlin-3 deletion, marginal zone B cells are lost while follicular B cells are expanded

Having observed that both CD49d integrin and its intracellular adaptor K3 are mandatory to ensure normal IgM high and IgD low expressing (IgM^{high}/IgD^{low}) immature as well as recirculating, mature B cell numbers in BM (Figure 1 Cii,D), we next analyzed whether these subsets are altered in the blood of K3ΔB and CD49dΔB mice. In K3ΔB mice, the immature and mature B cell pools were homogeneously increased in the blood (Figure 2A), which was reflected in an elevation of total B cell numbers (Supplemental Fig. 2A). CD49dΔB mice did not exhibit this increase in blood B cells, suggesting that CD49d is not the only integrin controlling the trafficking of this pool of B cells.

Spleen weight was significantly increased in K3ΔB compared to wt controls (Figure 2B). We visualized splenic structures by using immunofluorescence (Figure 2C) as well as immunohistochemical approaches (Supplemental Fig. 2B, C). Laminin immunofluorescence staining of spleen sections combined with B220 as a B cell marker revealed the lack of loosely packed marginal zone (MZ) B cells surrounding the quasi-continuous laminin staining lining of the white pulp[30] in K3ΔB mice. We confirmed this observation by using an Ab against metallophilic macrophages (Moma1, Figure 2C) to define the MZ, in combination with IgM. Metallophilic macrophages form a ring around the follicular areas at the inner side of the MZ. In all staining approaches, MZ B cells lined the white pulp areas in wt mice but were absent in K3ΔB mice (Figure 2C; the MZ is indicated by double arrows in the wt and CD49dΔB panels, single arrows show the MZ area lacking MZ B cells in the K3ΔB panel). In CD49dΔB spleens, the MZ B cell compartment was thinner than in wt mice but still present. This phenotype

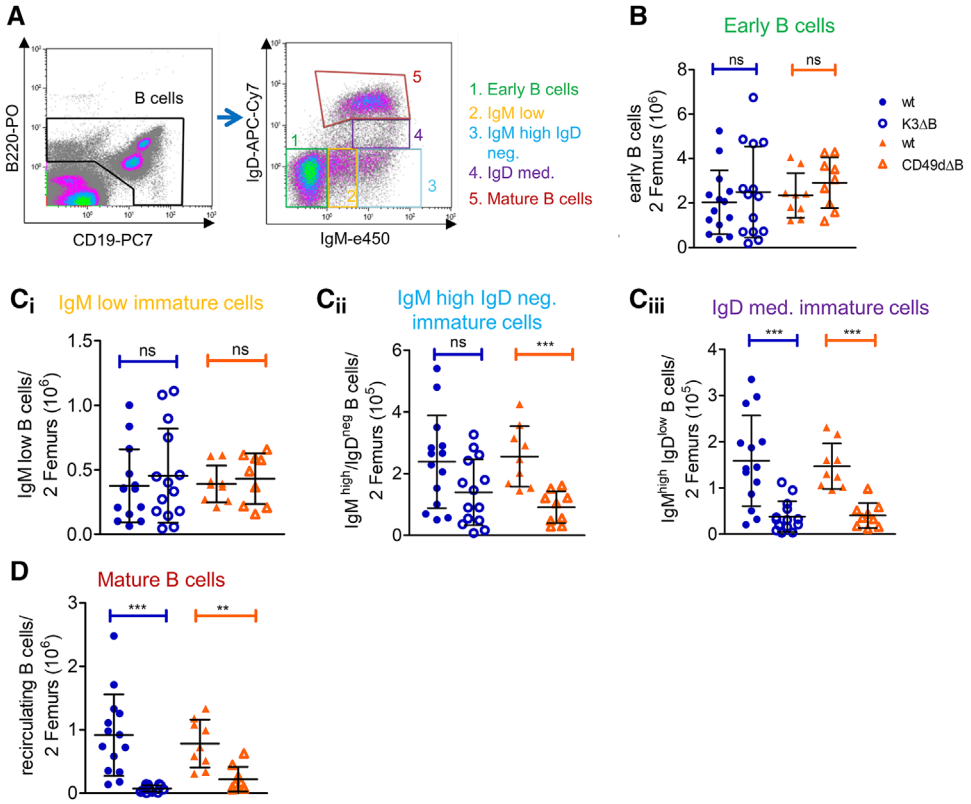

FIGURE 1 **K3 and CD49d are equally important for developing B cell subsets in BM.** BM-derived B cells were defined as B220 and/or CD19 positive as shown by an exemplary flow cytometry plot of a wt mouse. B cell developmental stages were defined by IgM and IgD expression **(A)**. K3ΔB mice (n = 14 per group), CD49dΔB mice (n = 9 per group) were compared to their respective Cre negative wt littermates. Early B cells (green gate) were defined as IgM/IgD negative **(B)**. Immature B cell populations were subdivided according to the expression levels of IgM and IgD (orange, blue and purple gates and plots **(Ci-Ciii)**. Recirculating B cells (red gate) were IgM and IgD high **(D)**, groups were compared using unpaired *t*-test. ns: $P > 0.05$; $^{**}P < 0.01$; $^{***}P < 0.001$

was confirmed by immunohistochemistry, revealing a sharper boundary between B cell follicles and red pulp in K3ΔB than in control mice (Supplemental Figure 2 B, C), and a reduced thickness of the MZ B cell area in most of the follicles of CD49dΔB mice.

Next, we analyzed the composition of splenic B cell subsets by flow cytometry, confirming that MZ B cells were absent in K3ΔB mice. In CD49dΔB mice, MZ B cell numbers were significantly reduced compared to wt (Figure 2D). In contrast, total spleen numbers of immature, transitional B cell were unaffected by the knockout conditions (Figure 2Ei). In K3ΔB mice, a strong increase in mature, follicular B cells was observed (Figure 2Eii).

3.3 | Upon Kindlin-3 deletion B cells home preferentially to spleen

We next delineated the mechanisms of MZ B cell abrogation and follicular B cell expansion upon K3 loss. First, to test the recirculation and homing capacity of splenic cells, we crossed K3ΔB mice with mice expressing a fluorescent reporter for Cre activity.[31] In this reporter system, B cells expressed eGFP in the presence of Cre, while cells with no active Cre expressed tdTomato (Supplemental Fig. 3A). This system allowed detection of the knockout and wt cells in a short-term (i.e., 3 h) homing assay. In accordance with the elevated B cell numbers in the spleen in K3ΔB mice (Figure 2B), the total spleen homing rate of K3 deficient B cells was significantly increased, to 1.8 times the rate of wt B cells. The fraction of K3-deficient B cells remaining in the blood was increased 3.3-fold, compared to their controls. Recirculation to BM was strongly reduced to only 6.7% of the homing rate of K3-proficient B cells (Figure 3A).

Described key factors mediating B cell homing to and localization within spleen are the chemokine receptors CXCR4 and CXCR5,[32] and the adhesion molecule CD44,[33,34] besides the integrins VLA-4 and LFA-1. Analyzing their expression on spleen-derived B cells in the presence and absence of K3, CXCR5, and CD44 expression was significantly increased in K3 deficient B cells, and CXCR4 expression was retained (Figure 3B). VLA-4 and LFA-1 subunits (CD49d, CD29, CD11a, CD18) were comparable in K3 deficient and proficient splenic B cells (Figure 3C). In CD49dΔB mice, the only significant change observed (besides the obvious loss of CD49d, Supplemental Fig. 1B) was the concomitant downregulation of its beta subunit CD29 (Supplemental Fig. 3B). Collectively, the data suggest that defective integrin function in K3-deficient B cells is accompanied by an altered requirement and function of the chemokine (CXCR5)-CD44 axis.

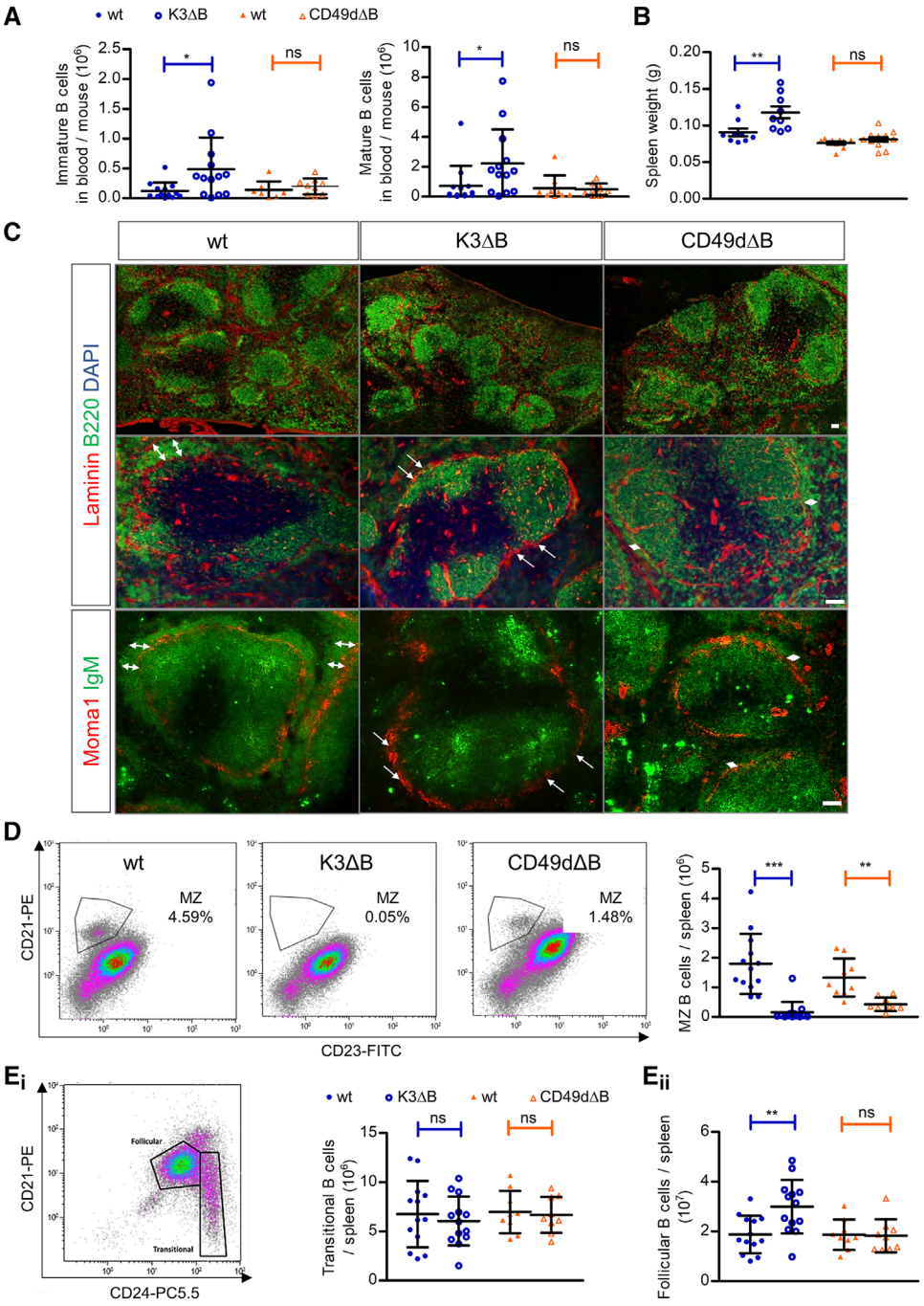

FIGURE 2 **MZ B cells are lost and follicular B cells expanded in the absence of K3, while CD49dΔB mice merely show reduced MZ thickness.** Heart blood from K3ΔB mice (n = 13 per group), CD49dΔB mice (n = 9 per group) and respective wt littermates was analyzed by flow cytometry. Immature B cells were defined by high IgM and low/no IgD expression, while mature B cells expressed high levels of IgD **(A)**. Spleens were isolated and weighed **(B)**. Cryosections of spleens were stained with Abs against Laminin and B220 defining follicle boundaries and B cell zones respectively (upper panels) or Moma1 and IgM defining metallophilic macrophages and B cell zones respectively (lower panel). White double arrows indicate the width of the MZ, the single arrows in the K3ΔB panels indicate where the marginal zone is absent. Scale bars depict 50 μm **(C)**. MZ B cells were flow cytometrically assessed by gating on the CD21high/CD24low population. Representative dot plots and quantification of MZ B cells are shown here **(D)**. Transitional **(E_i)** and follicular **(E_{ii})** B cells were defined by expression levels of CD21 and CD24 as shown. Groups were compared using unpaired t-test. ns: $P > 0.05$; *: $P < 0.05$; **: $P < 0.01$; ***: $P < 0.001$

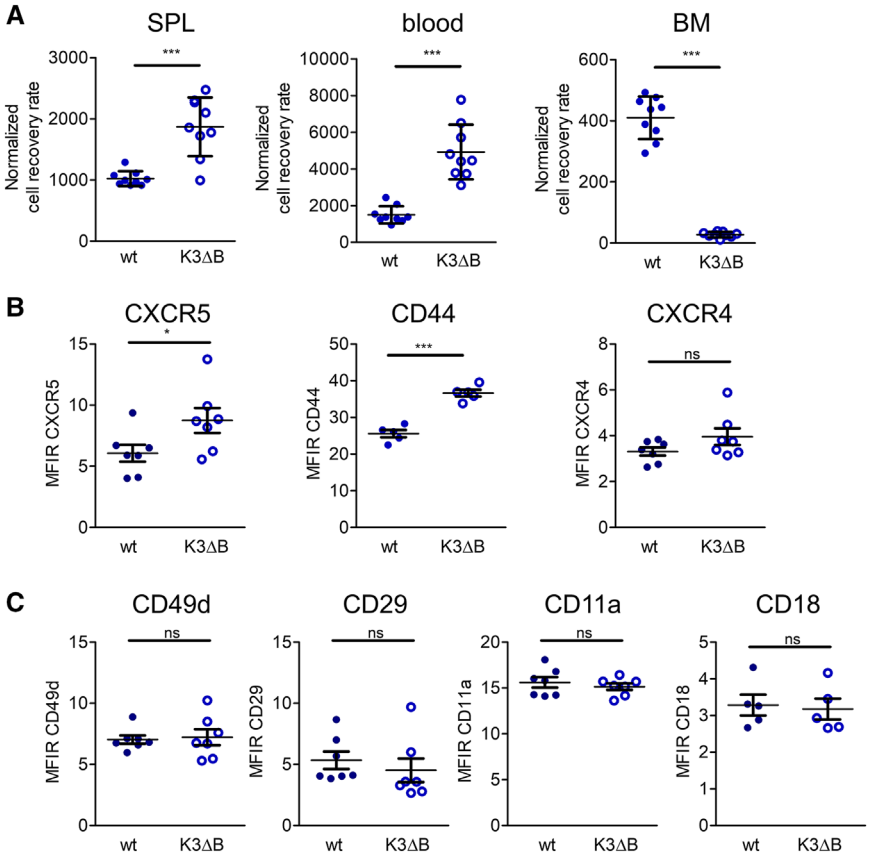

FIGURE 3 **K3 deficient B cells show altered homing and homing receptor expression, and MZ B cell retention in the spleen is dependent on K3**. Splenocytes were isolated from K3 fl/fl Cre reporter mice ± mb1 Cre and injected into the tail vein of wt C57BL/6 mice. After 3 h, spleen, blood, and BM of the recipients were analyzed by flow cytometry. B cells were identified by CD19 and T cells by CD5 expression, transferred cells were identified by red/green fluorescence. The normalized cell recovery rate was calculated as transplanted cells per million of total cells per million cells injected (n = 9 per group) **(A)**. Receptor expression was analyzed by flow cytometry on whole splenocytes of K3ΔB mice and control littermates. B cells were defined by CD19 expression **(B)** and **(C)**. Groups were compared using unpaired t-test. ns: $P > 0.05$; $^{*}P < 0.05$; $^{***}P < 0.001$

3.4 | Chemokine- and BCR-mediated integrin activation is highly dependent on K3

To confirm the presumable defect in chemokine-induced integrin activation in K3-deficient B cells, we used a real-time binding assay based on the small monovalent VLA-4 ligand LDV,[23] coupled to a fluorophore (FITC), as described.[22] The rate at which bound LDV-FITC is replaced by unlabeled competing LDV is a direct measure of the affinity state of the VLA-4 integrin and allows for calculation of dissociation constants and the reciprocal ligand residence time.[23,24] Stimulation of the CXCR4 receptor by CXCL12 (Figure 4A), or the CXCR5 receptor by CXCL13 (Figure 4B) doubled ligand residence time from about 12 s to 24 s, reflecting a switch from low to medium affinity VLA-4.[23] Both chemokines failed to increase VLA-4 affinity in K3-deficient B cells.

Integrin activation of B cells interacting with follicular dendritic cells might involve B cell receptor stimulation by Ag, which is presented by the follicular dendritic cells, along with integrin ligands and chemokines. In wt but not K3-deficient cells, B cell receptor stimulation by anti-IgM increased VLA-4 affinity comparable to chemokine-mediated activation (Figure 4C). To demonstrate that not only VLA-4 but also LFA-1 activation on B cells is defective upon K3 loss, we used a reductive assay under shear flow mimicking homing processes, as previously described.[17,22] Thereby, inside-out activation of VLA-4 or LFA-1 by CXCL12 takes place in vitro when cells are allowed to interact with adhesive surfaces coated with VCAM-1/ICAM-1 and CXCL12.[35] In this assay, in the absence of the stimulatory chemokine signal, only a few cells arrested (Figure 4D, E). Arrests were strongly increased in presence of the chemokine and clearly required the presence of K3, suggesting its contribution for VLA-4 and LFA-1 inside-out activation to high-affinity states.

Integrin-mediated adhesion and retention are most relevant to cell populations at tissue-circulation interfaces, as is the spleen MZ. However, inhibition or alteration of normally long-lasting integrin-mediated signals could also contribute to the shifted B cell populations in K3 knockout mice. To differentiate between rapidly induced and slowly developing defects in the absence of K3, we used a tamoxifen-inducible K3 knockout mouse strain (Fermt3fl/fl RosaCreERT2 mice).[13] One week after knockout induction, a significant population of MZ B cells was found in the blood of tamoxifen-treated, but not control-treated animals. 2 weeks after treatment, this population was no longer detectable (Figure 4F). In the spleen, the loss of K3 reduced the MZ B cell population to about 20% of the numbers found in control mice (Figure 4G). In summary, the data demonstrate that K3 is indispensable for inside-out activation of VLA-4 and LFA-1 integrins on splenic B cells, which in turn are required for homing and retention of shear force-experiencing B cells, particularly MZ B cells. In contrast, follicular B cells were unaltered in this short-term inducible K3 knockout mouse model (Figure 4H), indicating a long-term cause for follicular B cell expansion.

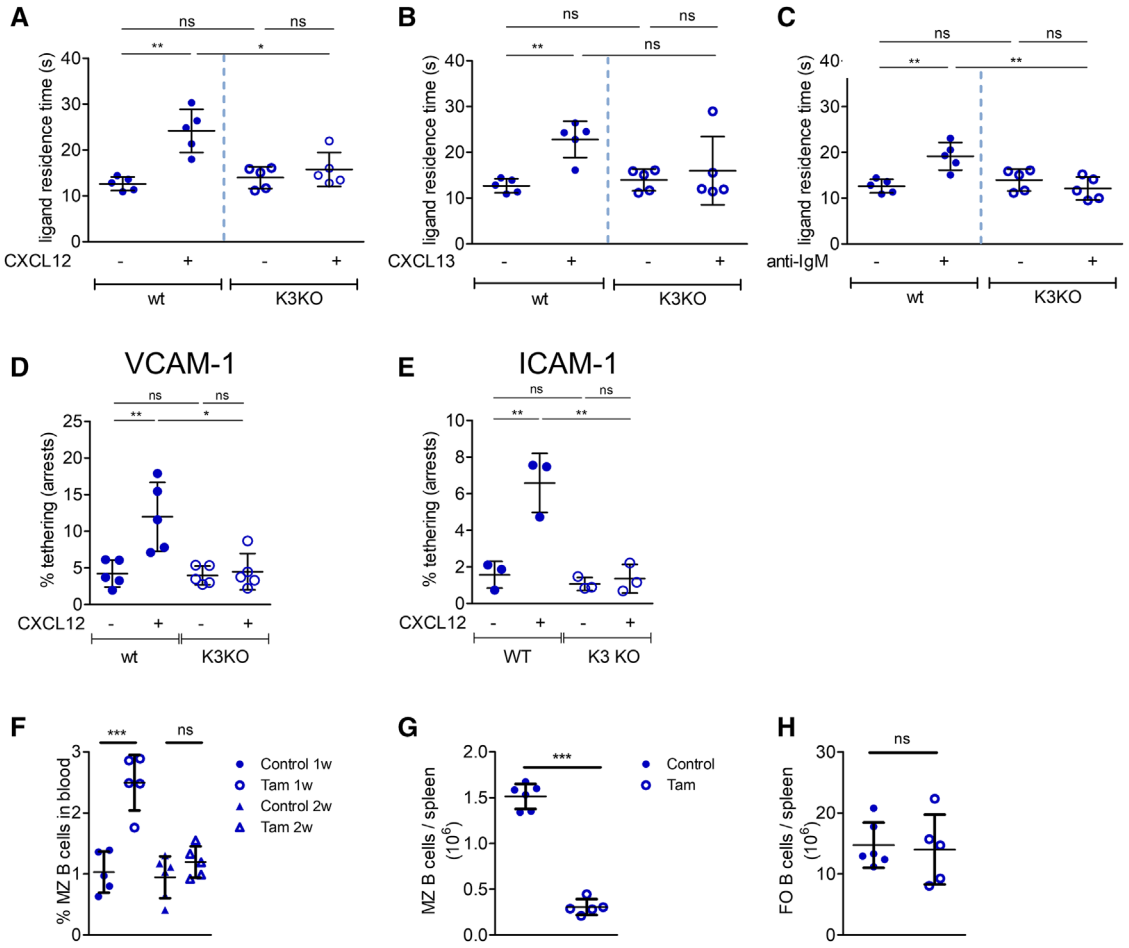

FIGURE 4 **K3 is indispensable for VLA-4 inside-out activation.** To determine VLA-4 affinity state, real time kinetic measurements were performed on B cells isolated by negative selection as described in.[23] A ligand residence time below 17 s indicates low affinity VLA-4, between 17 s and 50 s intermediate affinity and above 50 s high affinity. CXCL12 **(A)**, CXCL13 **(B)**, or anti-IgM F(ab)$_2$ **(C)** were added to stimulate VLA-4 affinity upregulation (n = 5). Negatively selected B cells were perfused over a VCAM-1 **(D)** (n = 5) or ICAM-1 **(E)** (n = 3) coated surface with or without co-immobilized CXCL12 K3 fl/fl - Rosa26CreERT2 mice were treated with 5 mg Tamoxifen (Tam) on two consecutive days. Control mice were treated with oil (n = 5 per group). One (1w) and 2 weeks (2w) after treatment, MZ B cells were detected in the peripheral blood by flow cytometry **(F)**. Two weeks (2w) after the treatment, the spleen was analyzed by flow cytometry for the content of MZ **(G)** and follicular **(H)** B cells. Groups were compared using unpaired *t*-test. ns: $P > 0.05$; $^{*}P < 0.05$; $^{**}P < 0.01$; $^{***}P < 0.001$.

3.5 | K3 deficient follicular B cells display a signature of increased activation and are prone to proliferate

To get insights into the causes for the increase in follicular B cell numbers, we sorted this population from the spleens of K3ΔB and control mice (Supplemental Figure 4A) and performed a transcriptome array. A linear based-model differential analysis showed 263 genes to be significantly ($P < 0.05$) up-regulated in Kindlin-3 deficient compared to control B cells, while only 41 genes were significantly downregulated (Supplemental Figure 4B). Among the 50 most significantly regulated genes, shown in Figure 5A, were the chemokine receptor CXCR5 and several important signaling molecules. Gene set enrichment analysis (GSEA) showed an upregulation of central signaling pathways such as BCR and NF-kappaB signaling (Figure 5B) in K3 deficient B cells. The most significantly regulated gene sets from the used databases are shown in Supplemental Fig. 4C. The increased activity of these pathways, together with metabolic changes exemplified by increased activity of the PI3K-AKT-MTOR pathway and upregulation of oxidative phosphorylation genes (Fig. 5C) show a generally increased activation state of the K3 deficient follicular B cells.

Confirming the phenotype of increased activation, CD69, CD40, CD38, CD44, CXCR5, and EBI2 mRNA levels were upregulated (Supplemental Fig. 5A) and protein surface expression (CXCR5, CD44: Figure 3; CD69, CD40: Figure 6A) was increased in K3 deficient follicular B cells. These molecules are associated with Ag-driven germinal center (GC) responses and contribute to plasmablast differentiation.[36–38] During an immune reaction, activation via the BCR and CD40 on follicular B cells results in selective expansion of reactive B cells. Thus, we stained spleen cryosections for the proliferation marker Ki67 and

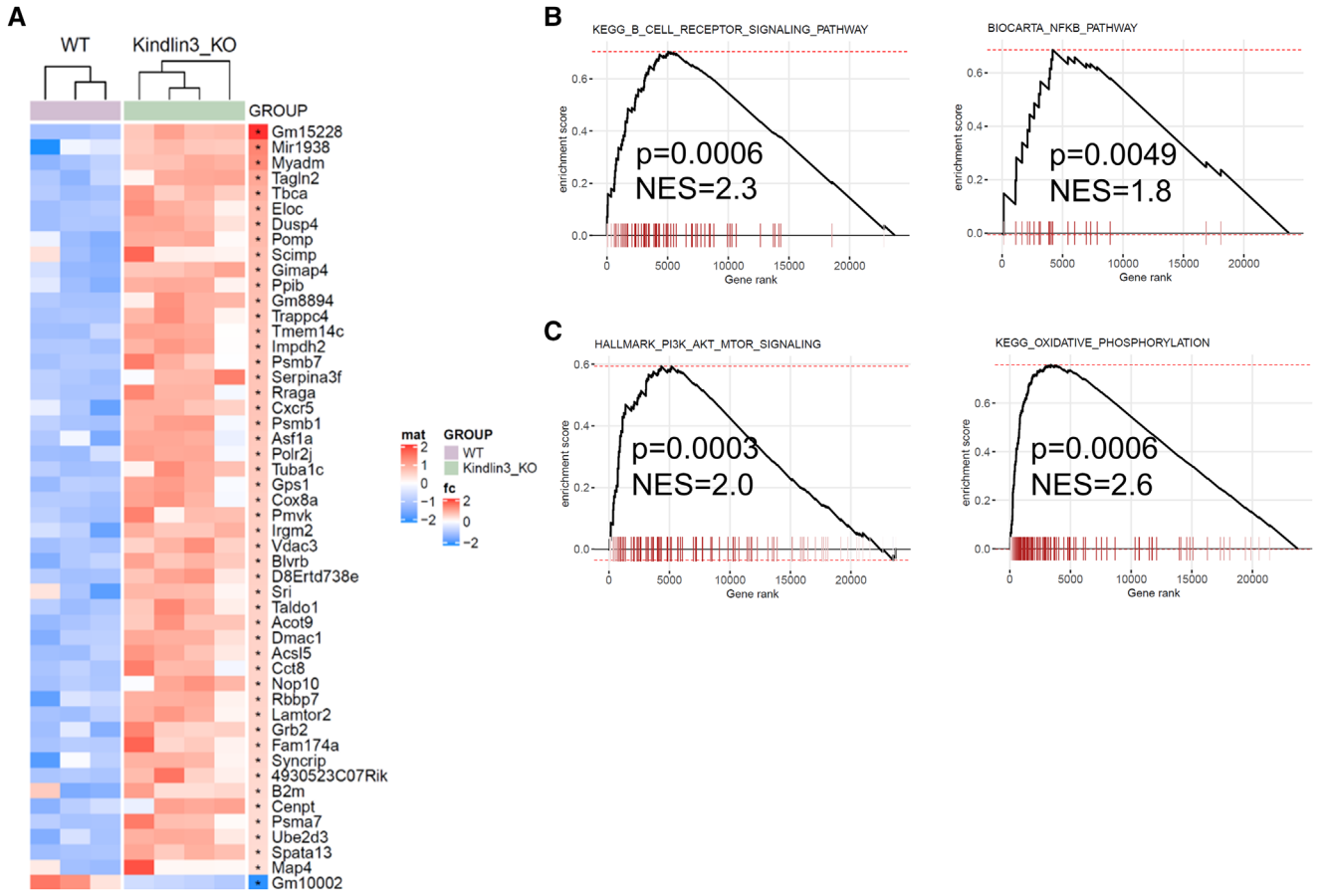

FIGURE 5 **K3 deficient follicular B cells display an activation phenotype on RNA and surface receptor level.** Follicular B cells were sorted from the spleens of K3ΔB (n = 4) mice and control littermates (n = 3). Row-wise scaled (*Z*-score, color-coded) heatmap of the top 50 regulated genes between K3 deficient B cells and control. Right column represents the log2 fold change and significantly regulated genes are highlighted by a "*" **(A)**. Gene set enrichment analysis was performed using several published databases from MSigDB. Enrichment plots show up-regulated gene-sets in K3 deficient B cells. Genes are ranked according to the log2 fold change in K3 deficient B cells vs. control (*X*-axis). Genes belonging to the respective gene-sets are showed with red ticks. The *Y*-axis shows the evolution of the enrichment score during the random walk over the ranked list of genes **(B and C)**

visualized the follicular architecture and B cell areas by co-staining of laminin and B220 (Figure 6B). In the spleens of wt littermate controls only few follicles showed clusters of proliferating cells, as expected in mice neither immunized nor exposed to pathogens. In contrast, in K3ΔB mice, clusters of proliferating cells could be found in the majority of follicles (Figure 6B). Quantification of the Ki67 positive cells revealed a specific increase of proliferating B cells in K3ΔB mice, while proliferation in the T-cell areas was unchanged (Figure 6C). In accordance with this, the numbers of CXCR5 positive follicular helper T cells (TFH) as well as co-stimulatory molecules on B cells (CD80, CD86) were unaffected by the K3 loss (Supplemental Fig. 5B and data not shown).

3.6 | K3ΔB mice show increased germinal center B cell and plasmablast numbers

Next, we characterized the possibility of a K3 loss-induced GC induction. Indeed, the absolute number of GC B cells (defined as $CD95^{high}CD38^{low}$, Figure 7A) was significantly increased in K3ΔB mice compared to wt littermates. We also observed an increase in plasmablasts ($TACI^{+}/CD138^{+}/B220^{high}/CD19^{low}$, Figure 7B, Supplemental Figure 6A) but not later stages of plasma cells (Supplemental Figure 6B), in line with our observation of an upregulation of the homing receptor EBI2 (Supplemental Figure 5A). For further in situ characterization of GC and class switched B cells, we stained spleen sections of K3ΔB mice and wt littermates for Ki-67 in combination with PNA, GL7 or IgG, to determine GC and class switched B cells, respectively. K3ΔB mice displayed an increase in Ki-67, PNA, GL7, and IgG positive areas (Figure 7C–E). We observed a significant increase in $PNA^{+}Ki67^{+}$ GC numbers in K3ΔB mice compared to wt littermates, with an intermediate GC number in K3ΔB mice (around 2 GCs/mm^2, Figure 7C). Thereby, Ki-67 positive clusters overlapped with GL7 (Figure 7D); IgG positive areas were located adjacent to the main proliferative areas (Figure 7E). Further, proliferating B cells partially expressed high IgM levels (Supplemental Fig. 6C). Our data suggest that absence of K3 triggers an expansion of follicular B cells and enhances their commitment to differentiate into GC B cells and plasmablasts.

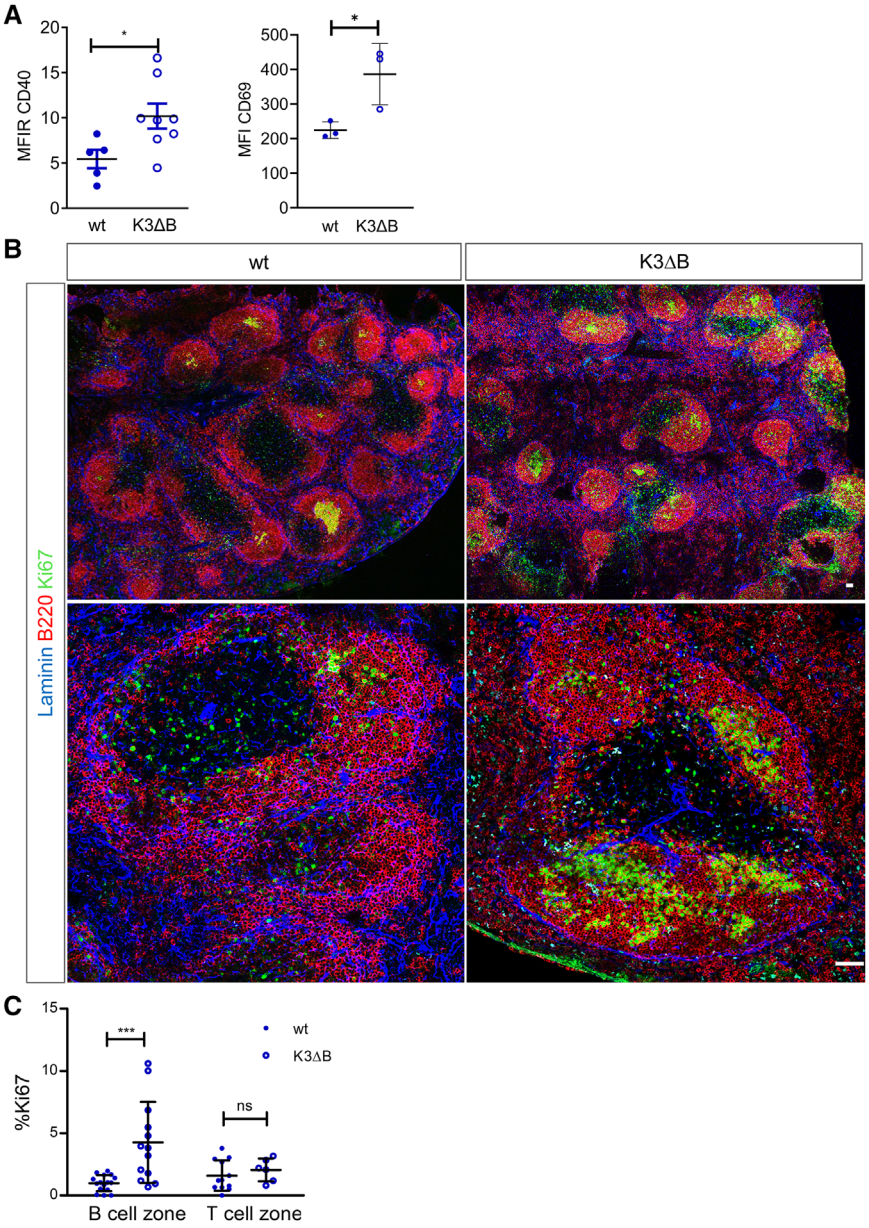

FIGURE 6 **K3ΔB mice show an increase in proliferation centers in splenic follicles**, CD40 and CD69 expression of follicular B cells of K3ΔB and control mice was determined by flow cytometry (n = 5 wt; n = 7 K3ΔB for CD40 and n = 3 in both groups for CD69) **(A)**. Cryosections of spleens from K3ΔB and control mice were stained with Abs against Laminin (blue) to mark white pulp boundaries, B220 (red) to define B cell zones and Ki67 (green) as a marker for proliferating cells. Scale bars are 50 μm **(B)**. Quantification was done using ImageJ by manually defining B- and T-cell zones based on laminin and B220 staining. The total and Ki-67 positive areas of B- or T-cell zones were measured and the Ki-67 positive fractions were calculated (one representative of 3 analyzed pairs of littermates is shown, 7 images were counted per spleen) **(C)**. Groups were compared using unpaired *t*-test. ns: $P > 0.05$; $^{*}P < 0.05$; $^{***}P < 0.001$

3.7 | K3 deletion specifically increases the response of follicular B cells to CXCL13 and IgD activation

To identify the causes for the observed proliferation and lineage skewing of K3 deficient follicular B cells, we assessed the expression of the BCR IgD and IgM isotypes and found significantly elevated IgD but unaltered IgM on these cells, compared to K3 proficient cells (Figure 8A). We analyzed calcium (Ca2+) mobilization upon BCR as well as CXCR4 and CXCR5 (compare Figure 3B) stimulation. An example of the analysis is depicted in Supplemental Fig. 7A. While we found comparable calcium responses to anti-IgM, anti-kappa light chain and IgD activation in K3 deficient and wt follicular B cells (Supplemental Fig. 7B), the Ca2+ response to CXCL13, but not CXCL12 was increased in K3 deficient B cells (Figure 8B). These data proposed an increase in CXCR5 responsiveness, in line with the increased CXCR5 but retained CXCR4 expression (Figure 3B). To further corroborate this finding, we next analyzed activation of the PI3K pathway in response to CXCL13 and anti-IgD stimulation, using a phosphoflow approach for the PI3K target Akt. In accordance with the Ca2+ data, Akt phosphorylation in response to CXCL13, but not α-IgD was increased in K3 deficient follicular B cells (Figure 8C). Along this line, CXCL13-induced chemotaxis was retained in K3 deficient follicular B cells despite their lower general and CXCL12-induced motility (Figure 8D). We confirmed this observation on a collagen substrate with or without co-immobilized CXCL12 or CXCL13. In line with this finding, polarization of the actin cytoskeleton during migration on a collagen substrate, as analyzed by phalloidin staining, was significantly increased in the presence of CXCL13 but not CXCL12 in K3 deficient B cells (Figure 8E, Supplemental Fig. 7C). In summary, we observed a clear preference of K3 deficient B cells for CXCR5 over CXCR4 signals and signs of altered motility, consistent with GC formation.[36,39]

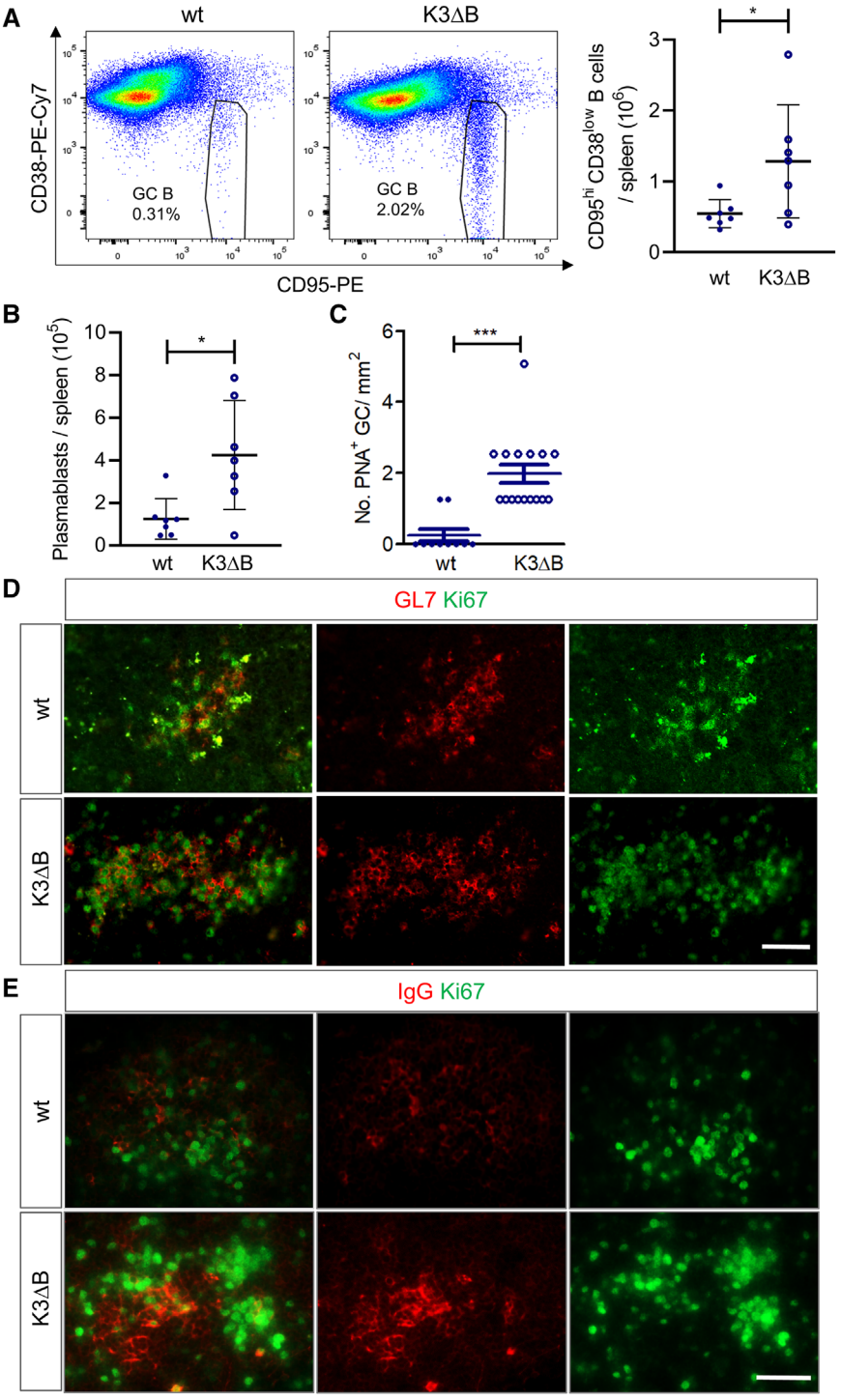

FIGURE 7 **K3ΔB mice show an increase in GC B cells and plasmablasts**, GC B cells were flow cytometrically defined as $CD95^{high}$ $CD38^{low}$ (pre-gated on CD19 positive) in the spleens of K3ΔB and control mice as shown (n = 7) **(A)**. Plasmablasts numbers were determined by flow cytometry as $TACI^{+}/CD138^{+}/B220^{high}/CD19^{low}$ (n = 7) **(B)**. Cryosections of spleens from K3ΔB and control mice were stained for PNA/ GL7 (red) to mark germinal centers **(C, D)**, or IgG (red) to mark class-switched B cells **(E)**, together with Ki67 (green) defining proliferating cells. Scale bars are 50 μm. PNA^{+} germinal centers (GCs) were quantification in K3ΔB and control mice **(C)**. Groups were compared using unpaired *t*-test. ns: $P > 0.05$; $^{*}P < 0.05$; $^{***}P < 0.001$

4 | DISCUSSION

In this study, we analyzed B-cell intrinsic functions of the integrin adaptor K3 and one of the major B cell integrins, VLA-4 (CD49d), on basis of highly specific conditional knockout mouse models. We found that MZ B cell retention relies entirely on functional K3 and partially on VLA-4. We also provide evidence that K3-mediated signaling serves as a monitor of the follicular B cell pool, by limiting their proliferation and further differentiation, via controlling their CXCR5 responsiveness.

MZ B cells are a specialized splenic B cell subset cycling between sinusoids and white pulp.[40] These cells are prone to disturbances by dual VLA-4 and LFA-1 integrin blockage and rely on several factors involved in stabilization of high affinity adhesive processes.[41,42,43] In K3ΔB mice, we observed a loss of MZ B cells and nonfunctional inside-out activation of both, VLA-4 and LFA-1 integrins. Our data suggest that K3 abrogation directly interferes with integrin-mediated retention of B cells in the MZ, which we confirmed by use of a tamoxifen-inducible knockout model that mobilized MZ B cells into blood. The

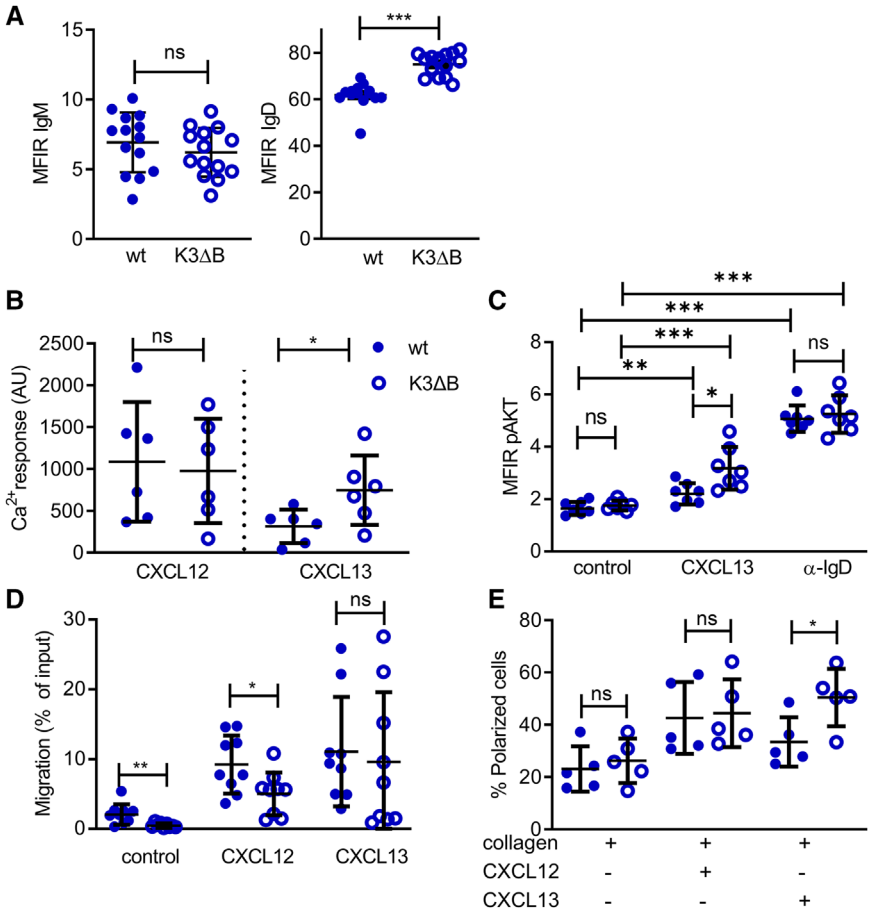

FIGURE 8 **K3ΔB mice show increased signaling capacity towards CXCR5 activation and altered migration behavior**, IgM and IgD levels were determined by flow cytometry on follicular B cells of K3ΔB and control mice ($n = 14$ per group) **(A)**. Fluo-3 loaded splenocytes were stimulated with CXCL12 or CXCL13 ($n = 6$ per group) to induce calcium mobilization. **(B)**. Splenocytes of K3ΔB and control mice were stimulated with CXCL13 and α-IgD for 5 min, and Akt phosphorylation was determined by flow cytometry (n = 7 per group) **(C)**. Splenocytes of K3ΔB and control mice were subjected to a transwell migration toward medium alone (control), CXCL12, or CXCL13 (n = 9 per group) **(D)**. Negatively selected B cells from K3ΔB and control mice were seeded on a substrate of Collagen I alone or co-coated with CXCL12 or CXCL13. F-actin was stained with Phalloidin-AF488, images were taken at Zeiss AxioObserver (20× magnification) and cells were manually classified as polarized or unpolarized according to the pattern of phalloidin staining. Between 100 and 300 cells were counted per condition; dots represent 5 independent experiments **(E)**. Groups were compared using unpaired *t*-test. ns: $P > 0.05$; $^{*}P < 0.05$; $^{**}P < 0.01$; $^{***}P < 0.001$

adhesive cues necessary for MZ maintenance depend in part on VLA-4, as loss of CD49d reduced but not completely abrogated MZ B cells. Our findings are consistent to the report that MZ B cells adhere and migrate with the flow in a VLA-4-VCAM-1 dependent manner and utilize LFA-1 for migration against the flow.[44] Our mouse models also reflect the co-dependency of MZ B cells on both integrins that has recently been suggested on basis of Ab-blocking experiments.[42]

Both, absence of K3 and CD49d caused a massive reduction of $IgM^{+}/IgD^{neg/low}$ immature B cells in the BM, arguing for VLA-4 as the major integrin regulated by K3 activity in immature B cells. These cells normally reside in the BM sinusoidal vessels and the parenchyma in a VLA-4-VCAM and CXCR4-CXCL12 dependent manner.[29,45] In consistence, we observed a reduced B cell chemotaxis to CXCL12 when K3 expression was abrogated.

In contrast to two previous reports[46,47] we clearly show that K3 is required for inside-out VLA-4 activation. This activation cascade integrates signals from the microenvironment such as chemokines or Ag, and is therefore highly relevant for B cell differentiation. Notably, only by using models harboring a complete knockout of K3, as achieved in our conditional knockout mice, residual activity of K3 is excluded. This is crucial, as a minimal amount of K3, which is present in knockdown approaches, is sufficient to enable integrin activation,[48] which might explain the discrepancy to previously reported observations.

An unexpected finding was the markedly enhanced proliferation of follicular B cells and the enrichment of GC B cells and plasmablasts in K3ΔB mice. Obviously, K3-mediated signaling serves as a control point for follicular B cell fate, while CD49d is not sufficient for this function. One possible explanation is that the total loss of integrin-mediated signals and adhesion sites in the K3 KO influences the cytoskeleton (see Figure 8E), thereby altering membrane compartmentalization and BCR–co-receptor cooperation.[49] Lack of K3 also results in unoccupied focal adhesion molecules, which could be sequestered to and function in the nucleus.[50,51] In addition, K3 might also fulfill adaptor functions independent of integrin cytoplasmic tails.[52] The K3 interactome and K3-controlled signaling pathways in follicular B cells remain, however, to be elucidated in future projects.

Besides retention, the numbers of mature B cell subsets in spleen are determined by their continuous differentiation from BM-derived immature progenitors and their subsequent survival and proliferation within the spleen microenvironment. All these processes depend on activation signals received through the B cell receptor.[53] Our transcriptome analysis of K3 knockout follicular B cells showed an upregulation of essential B cell differentiation and signaling pathways, that is, the BCR pathway, MAPK- and NF-kappaB pathways and revealed increased expression of oxidative phosphorylation genes,[54] pointing to an activation phenotype of K3 knockout follicular B cells. As the observed activation signatures are normally a consequence of Ag encounter during an immune reaction, K3 deficient B cells may either possess an altered BCR activation threshold, or their BCR repertoire or signaling cascades are altered to receive more activation. In line

with this hypothesis, we found increased surface expression of IgD and CD40. Moreover, K3 loss enhanced EBI2 transcription and CXCR5 responsiveness, and therefore induced plasmablast differentiation and a spontaneous but dispersed germinal center formation. Usually, activated B cells are recruited to CXCL13-expressing follicular dendritic cells, where they are supported by tightly regulated adhesive interactions with this microenvironment,[36,39,55,56] which allows their further differentiation. Without K3, the coordinated process of BCR stimulation, adhesion to follicular dendritic cells, and T cell support appears to be disrupted.

In summary, besides providing mechanistic insights into the VLA-4-dependency of immature and LFA-1/VLA-4 dependency of marginal zone B cells, we found a novel contribution of K3 in limiting and controlling follicular B cell activation, proliferation in spleen and commitment toward germinal center responses, by altering their CXCR5 responsiveness, and thus their localization and further interaction with the spleen microenvironment.

ACKNOWLEDGMENTS

We are grateful to the Lighthouse Core Facility (M. Follo and team) for the most valuable continuous support and technical assistance with flow cytometry and cell sorting. We thank Ronen Alon for helpful discussion and advice. We thank Alexandre Chigaev for the gift of the LDV peptide and continuous advice and support. We thank Reinhard Fässler for the Fermt3 floxed mice, Thalia Papayannopoulou for the Itga4 floxed mice and Michael Reth for the Mb1 Cre mice. We thank Alexander Egle and Cornelius Miething for help with mouse administration, Daniela Asslaber and Julia Gutjahr for help with mouse dissection, and Alexandra Mühlthaler for mouse handling support. This work was supported by the Deutsche Forschungsgemeinschaft (DFG, German Research Foundation) 419090910 and 437764346 and the Deutsche Krebshilfe (DKH) 70113993 to T.N. Hartmann, the Austrian Science Fund (FWF) P26421 to T.N. Hartmann, the PhD program Immunity in Cancer and Allergy (W1213, Austrian Science Fund) to T.N. Hartmann, and a Paracelsus Medical University PMU-FFF grant to T.N. Hartmann, the SCRI-LIMCR GmbH, an unrestricted research support by Roche to R. Greil and the Deutsche Forschungsgemeinschaft, Germany for the SFB 850 and SFB1160 to M. Boerries (Z1). M. Boerries is supported by the German Federal Ministry of Education and Research for MIRACUM within the Medical Informatics Funding Scheme (FKZ 01ZZ1606B). P.W. Krenn is supported by the Biomed Center Salzburg (Project 20102-F1901165-KZP).

AUTHORSHIP

A.H., L.L., and T.N.H. designed the research concepts; P.W.K., R.R., and P.C.M. contributed to the research concepts; A.H., P.W.K., L.L., D.P., and S.T. developed methodology; A.H., L.L., P.W.K., E.S-N., E.B., L.P., U.D., J.P.H., E.K., D-J.D., S.T., and R.R. performed research; A.H., P.W.K., L.L., E.S-N., E.B., D.P., S.T., L.K., and M.B. analyzed data; A.H., P.W.K., and T.N.H. wrote the paper; L.L., G.A., L.P., S.T., M.B., R.R., and P.C.M. revised the manuscript; L.K., H.J., R.G., M.B., P.C.M., and T.N.H. provided scientific, administrative, technical or material support; T.N.H. supervised the study.

DISCLOSURE

The authors have declared that no conflict of interest.

ORCID

Peter W. Krenn https://orcid.org/0000-0002-8896-8387
Tanja Nicole Hartmann https://orcid.org/0000-0002-0377-7179

REFERENCES

1. Abram CL, Lowell CA. The ins and outs of leukocyte integrin signaling. *Annu Rev Immunol*. 2009;27:339-62.
2. Arroyo AG, Yang JT, Rayburn H, Hynes RO. Differential requirements for alpha4 integrins during fetal and adult hematopoiesis. *Cell*. 1996;85:997-1008.
3. Papayannopoulou T, Craddock C, Nakamoto B, Priestley GV, Wolf NS. The VLA4/VCAM-1 adhesion pathway defines contrasting mechanisms of lodgement of transplanted murine hemopoietic progenitors between bone marrow and spleen. *Proc Natl Acad Sci U S A*. 1995;92:9647-51.
4. Oostendorp RA, Dormer P. VLA-4-mediated interactions between normal human hematopoietic progenitors and stromal cells. *Leuk Lymphoma*. 1997;24:423-35.
5. Carrasco YR, Batista FD. B-cell activation by membrane-bound antigens is facilitated by the interaction of VLA-4 with VCAM-1. *EMBO J*. 2006;25:889-99.
6. Carrasco YR, Fleire SJ, Cameron T, Dustin ML, Batista FD. LFA-1/ICAM-1 interaction lowers the threshold of B cell activation by facilitating B cell adhesion and synapse formation. *Immunity*. 2004;20:589-99.
7. Gutjahr JC, Bayer E, Yu X, et al. CD44 engagement enhances acute myeloid leukemia cell adhesion to the bone marrow microenvironment by increasing VLA-4 avidity. *Haematologica*. 2021;106:2102-2113.
8. Harzschel A, Zucchetto A, Gattei V, Hartmann TN. VLA-4 Expression and Activation in B Cell Malignancies: functional and Clinical Aspects. *Int J Mol Sci*. 2020;21.
9. Tissino E, Benedetti D, Herman SEM, et al. Functional and clinical relevance of VLA-4 (CD49d/CD29) in ibrutinib-treated chronic lymphocytic leukemia. *J Exp Med*. 2018;215:681-697.
10. Calderwood DA, Campbell ID, Critchley DR. Talins and kindlins: partners in integrin-mediated adhesion. *Nat Rev Mol Cell Biol*. 2013;14:503-17.
11. Moser M, Legate KR, Zent R, Fassler R. The tail of integrins, talin, and kindlins. *Science*. 2009;324:895-9.
12. Ussar S, Wang HV, Linder S, Fassler R, Moser M. The Kindlins: subcellular localization and expression during murine development. *Exp Cell Res*. 2006;312:3142-51.
13. Ruppert R, Moser M, Sperandio M, et al. Kindlin-3-mediated integrin adhesion is dispensable for quiescent but essential for activated hematopoietic stem cells. *J Exp Med*. 2015;212:1415-32.
14. Moretti FA, Moser M, Lyck R, et al. Kindlin-3 regulates integrin activation and adhesion reinforcement of effector T cells. *Proc Natl Acad Sci U S A*. 2013;110:17005-10.
15. Moser M, Bauer M, Schmid S, et al. Kindlin-3 is required for beta2 integrin-mediated leukocyte adhesion to endothelial cells. *Nat Med*. 2009;15:300-5.
16. Moser M, Nieswandt B, Ussar S, Pozgajova M, Fassler R. Kindlin-3 is essential for integrin activation and platelet aggregation. *Nat Med*. 2008;14:325-30.
17. Hartmann TN, Grabovsky V, Wang W, et al. Circulating B-cell chronic lymphocytic leukemia cells display impaired migration to lymph nodes and bone marrow. *Cancer Res*. 2009;69:3121-30.
18. Hobeika E, Thiemann S, Storch B, et al. Testing gene function early in the B cell lineage in mb1-cre mice. *Proc Natl Acad Sci U S A*. 2006;103:13789-94.

19. Cohen SJ, Gurevich I, Feigelson SW, et al. The integrin coactivator Kindlin-3 is not required for lymphocyte diapedesis. *Blood*. 2013;122:2609-17.
20. Scott L M, Priestley G V, Papayannopoulou T, (2003) Deletion of alpha4 integrins from adult hematopoietic cells reveals roles in homeostasis, regeneration, and homing. *Mol Cell Biol* 23, 9349-60.
21. Brachtl, G, Sahakyan, K, Denk, U et al. (2011) Differential bone marrow homing capacity of VLA-4 and CD38 high expressing chronic lymphocytic leukemia cells. *PLoS One* 6, e23758.
22. Ganghammer, S, Hutterer, E, Hinterseer, E et al. (2015) CXCL12-induced VLA-4 activation is impaired in trisomy 12 chronic lymphocytic leukemia cells: a role for CCL21. *Oncotarget* 6, 12048-60.
23. Chigaev, A, Blenc, AM, Braaten, JV et al. (2001) Real time analysis of the affinity regulation of alpha 4-integrin. The physiologically activated receptor is intermediate in affinity between resting and Mn(2+) or antibody activation. *J Biol Chem* 276, 48670-8.
24. Tummino, PJ and Copeland, RA (2008) Residence time of receptor-ligand complexes and its effect on biological function. *Biochemistry* 47, 5481-92.
25. Carvalho, BS and Irizarry, RA (2010) A framework for oligonucleotide microarray preprocessing. *Bioinformatics* 26, 2363-7.
26. Ritchie, ME, Phipson, B, Wu, D et al. (2015) limma powers differential expression analyses for RNA-sequencing and microarray studies. *Nucleic Acids Res* 43, e47.
27. Liberzon, A, Birger, C, Thorvaldsdottir, H, Ghandi, M, Mesirov, JP, Tamayo, P (2015) The Molecular Signatures Database (MSigDB) hallmark gene set collection. *Cell Syst* 1, 417-425.
28. Korotkevich, G, Sukhov, V, Budin, N, Shpak, B, Artyomov, MN, Sergushichev, A (2021) *Fast gene set enrichment analysis*. 060012.
29. Beck, TC, Gomes, AC, Cyster, JG, Pereira, JP (2014) CXCR4 and a cell-extrinsic mechanism control immature B lymphocyte egress from bone marrow. *J Exp Med* 211, 2567-81.
30. Lokmic, Z, Lammermann, T, Sixt, M, Cardell, S, Hallmann, R, Sorokin, L (2008) The extracellular matrix of the spleen as a potential organizer of immune cell compartments. *Semin Immunol* 20, 4-13.
31. Muzumdar, MD, Tasic, B, Miyamichi, K, Li, L, Luo, L (2007) A global double-fluorescent Cre reporter mouse. *Genesis* 45, 593-605.
32. Schulz, O, Hammerschmidt, SI, Moschovakis, GL, Forster, R (2016) Chemokines and Chemokine Receptors in Lymphoid Tissue Dynamics. *Annu Rev Immunol* 34, 203-42.
33. Gutjahr, JC, Szenes, E, Tschech, L et al. (2018) Microenvironment-induced CD44v6 promotes early disease progression in chronic lymphocytic leukemia. *Blood* 131, 1337-1349.
34. Protin, U, Schweighoffer, T, Jochum, W, Hilberg, F (1999) CD44-deficient mice develop normally with changes in subpopulations and recirculation of lymphocyte subsets. *J Immunol* 163, 4917-23.
35. Hartmann, TN, Grabovsky, V, Pasvolsky, R et al. (2008) A crosstalk between intracellular CXCR7 and CXCR4 involved in rapid CXCL12-triggered integrin activation but not in chemokine-triggered motility of human T lymphocytes and CD34+ cells. *J Leukoc Biol* 84, 1130-40.
36. Allen, CD, Ansel, KM, Low, C et al. (2004) Germinal center dark and light zone organization is mediated by CXCR4 and CXCR5. *Nat Immunol* 5, 943-52.
37. Gatto, D, Paus, D, Basten, A, Mackay, CR, Brink, R (2009) Guidance of B cells by the orphan G protein-coupled receptor EBI2 shapes humoral immune responses. *Immunity* 31, 259-69.
38. Pereira, JP, Kelly, LM, Xu, Y, Cyster, JG (2009) EBI2 mediates B cell segregation between the outer and centre follicle. *Nature* 460, 1122-6.
39. Wu, BX, Zhao, LD, Zhang, X (2019) CXCR4 and CXCR5 orchestrate dynamic germinal center reactions and may contribute to the pathogenesis of systemic lupus erythematosus. *Cell Mol Immunol* 16, 724-726.
40. Cinamon, G, Zachariah, MA, Lam, OM, Foss, FW Jr, Cyster, JG (2008) Follicular shuttling of marginal zone B cells facilitates antigen transport. *Nat Immunol* 9, 54-62.
41. Manevich-Mendelson, E, Grabovsky, V, Feigelson, SW et al. (2010) Talin1 is required for integrin-dependent B lymphocyte homing to lymph nodes and the bone marrow but not for follicular B-cell maturation in the spleen. *Blood* 116, 5907-18.
42. Lu, TT and Cyster, JG (2002) Integrin-mediated long-term B cell retention in the splenic marginal zone. *Science* 297, 409-12.
43. Guinamard, R, Okigaki, M, Schlessinger, J, Ravetch, JV (2000) Absence of marginal zone B cells in Pyk-2-deficient mice defines their role in the humoral response. *Nat Immunol* 1, 31-6.
44. Tedford, K, Steiner, M, Koshutin, S et al. (2017) The opposing forces of shear flow and sphingosine-1-phosphate control marginal zone B cell shuttling. *Nat Commun* 8, 2261.
45. Pereira, JP, An, J, Xu, Y, Huang, Y, Cyster, JG (2009) Cannabinoid receptor 2 mediates the retention of immature B cells in bone marrow sinusoids. *Nat Immunol* 10, 403-11.
46. Hyduk, SJ, Rullo, J, Cano, AP et al. (2011) Talin-1 and kindlin-3 regulate alpha4beta1 integrin-mediated adhesion stabilization, but not G protein-coupled receptor-induced affinity upregulation. *J Immunol* 187, 4360-8.
47. Manevich-Mendelson, E, Feigelson, SW, Pasvolsky, R et al. (2009) Loss of Kindlin-3 in LAD-III eliminates LFA-1 but not VLA-4 adhesiveness developed under shear flow conditions. *Blood* 114, 2344-53.
48. Klapproth, S, Moretti, FA, Zeiler, M et al. (2015) Minimal amounts of kindlin-3 suffice for basal platelet and leukocyte functions in mice. *Blood* 126, 2592-600.
49. Kuokkanen, E, Sustar, V, Mattila, PK (2015) Molecular control of B cell activation and immunological synapse formation. *Traffic* 16, 311-26.
50. Dong, JM, Lau, LS, Ng, YW, Lim, L, Manser, E (2009) Paxillin nuclear-cytoplasmic localization is regulated by phosphorylation of the LD4 motif: evidence that nuclear paxillin promotes cell proliferation. *Biochem J* 418, 173-84.
51. Lim, ST, Miller, NL, Chen, XL et al. (2012) Nuclear-localized focal adhesion kinase regulates inflammatory VCAM-1 expression. *J Cell Biol* 197, 907-19.
52. Qu, J, Ero, R, Feng, C et al. (2015) Kindlin-3 interacts with the ribosome and regulates c-Myc expression required for proliferation of chronic myeloid leukemia cells. *Sci Rep* 5, 18491.
53. Loder, F, Mutschler, B, Ray, RJ et al. (1999) B cell development in the spleen takes place in discrete steps and is determined by the quality of B cell receptor-derived signals. *J Exp Med* 190, 75-89.
54. Waters, LR, Ahsan, FM, Wolf, DM, Shirihai, O, Teitell, MA (2018) Initial B Cell Activation Induces Metabolic Reprogramming and Mitochondrial Remodeling. *iScience* 5, 99-109.
55. Lu, E and Cyster, JG (2019) G-protein coupled receptors and ligands that organize humoral immune responses. *Immunol Rev* 289, 158-172.
56. Saez de Guinoa, J, Barrio, L, Mellado, M, Carrasco, YR (2011) CXCL13/CXCR5 signaling enhances BCR-triggered B-cell activation by shaping cell dynamics. *Blood* 118, 1560-9.

SUPPORTING INFORMATION

Additional supporting information may be found in the online version of the article at the publisher's website.

How to cite this article: Härzschel A, Li L, Krenn PW, et al. Kindlin-3 maintains marginal zone B cells but confines follicular B cell activation and differentiation. *J Leukoc Biol*. 2021;1–14. https://doi.org/10.1002/JLB.1HI0621-313R